High Resolution Models of Polar Ice Stability M. A. Siegler[1], J. Martinez-Camacho[2], David Paige[3], Jean-Pierre Williams[3], Mark Shirley[4], Ross Beyer[4], Masatoshi Hirabayashi[5], Richard Elphic[4], Emily Costello[6], Anthony Colaprete[4]
[1] Planetary Science Institute, [2] SMU. [3] UCLA, [4] NASA Ames, [5] Auburn U., [6] U. Hawaii

Introduction: The Lunar Prospector detection of hydrogen at the South Pole of the Moon [1] marked the beginning of a new era of lunar exploration. The idea that ice and other volatiles might be stable at the poles was not new [2], but had until then remained untested. Since this time, many of our efforts in lunar exploration have centered around mapping and explaining the origin of this hydrogen detection, believed to be water ice. Thermal models have been central to that discussion.

As the stability ice and other volatiles are exponentially dependent on temperature, understanding surface and subsurface temperatures is critical for locating where such deposits could be found. The LRO Diviner Lunar Radiometer has mapped surface temperatures at the poles to roughly 150 m resolution, but relies on models to extrapolate those surface conditions into the subsurface and fill in gaps in local time coverage [3].

Additionally, models can be pressed to much higher resolution than existing thermal measurements. The model is limited only by the existing elevation data. Both laser altimeter data (LOLA) and repeat visible imaging (LROC) can be used to produce digital elevation models. Shape-from-Shading (SfS) techniques have greatly advance in recent years, allowing for reliable topographic models to be made to nearly the resolution of instruments (~1m in the case of LROC WAC).

With the preparation for polar mission such and Viper, Artemis, and the CLPS and PRISM missions, several potential landing sites now have quality topographic data mapped to 1-5m resolution. This provides a great opportunity to map existing polar ice stability maps well beyond the existing 250m resolution map products [3,4] and the newly produced Diviner-based maps [5].

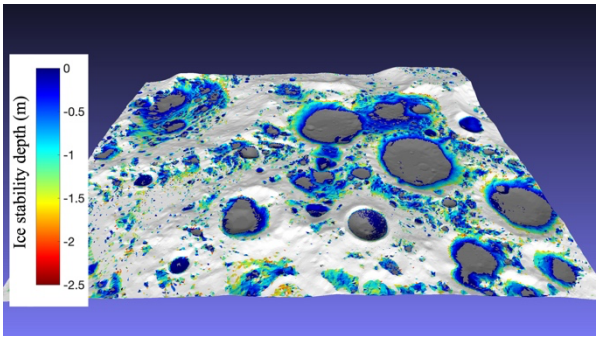

Figure 1: Modeled ice stability depth for a section of the lunar south polar region at ~80m (improving upon the existing 250m product from Paige et al., 2010, Siegler et al., 2016).

These models have been specifically pushed forward for use with the 2024 VIPER mission, where they are being used to aid in traverse and drilling planning to search for areas where water ice could be thermally stable. Thermal stability here means that it would sublimate at a rate of less than 1m per billion years. This is a somewhat arbitrary metric, but due to the exponential dependence of sublimation on temperature, it serves as an approximate marker of ice being stable over geologic times. If ice were delivered to these locations more recently, it could be found at shallower depths. If it was never delivered or moved by a non-thermal process, such as impact gardening [Hurley, Costello], it would also not necessarily be found at these predicted depths.

Just because ice is stable, it does not mean it is there. The ground truth of Viper will aid us in calibrating trends of how this ice stability criteria tracks with the actual presence of ice as a function of approximate surface age and apparent gardening depth. VIPER constraints on ice content with depth can then be related to models of episodic and continual water delivery.

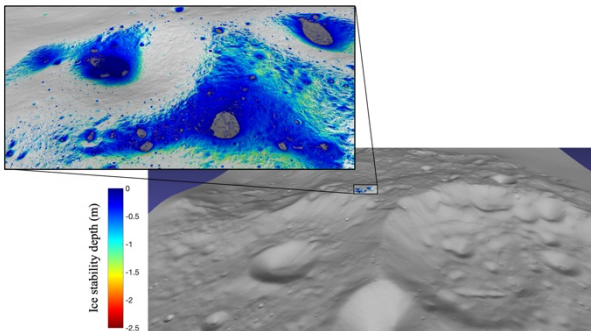

Figure 2: Model results for the Nobile region VIPER landing site at ~4m spatial resolution.

The Model: The thermal model is based on a heritage from models developed for the Diviner Lunar Radiometer on LRO [3,4,6]. These models use ray tracing between triangular facets to calculate the exchange of both visible and infrared radiation. The triangle facets can be made any size or proportion to model a given input topography. Triangles need not be the same size and can be decimated to allow lower resolution for terrain far from the region of interest.

Each triangle represents a 1D thermal model, nominally set to calculate 5mm thick layers to 2.5m depth. This model determines subsurface temperatures and infrared radiation between model facets. The Sun is treated as a distant disc composed of 128 triangles to give some fidelity of sunsets. The model nominally assumes Lambertian scattering of both visible and infrared light, but this is in the process of being updated.

Thermal properties are nominally from Hayne et al. [7] which outlines a temperature and density dependent thermal conductivity and specific heat capacity. Therefore, density is treated as a "master variable" which changes all other thermal quantities. New thermal model properties from Martinez et al. [8] have recently been added and may be more appropriate for temperatures below ~120K. Neither thermal or diffusive properties are updated with the presence of ice- the model always assumes dry regolith properties.

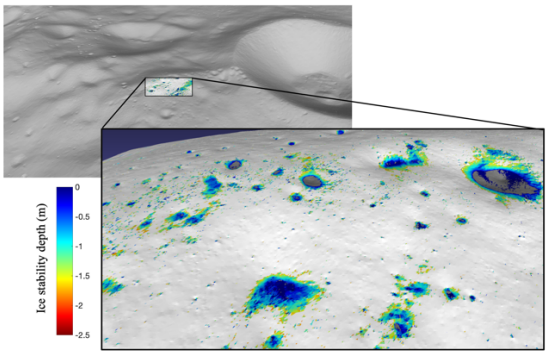

Figure 2: Model results for the "Shackleton Ridge" region, nominal PRIME-1 landing site at ~5m spatial resolution.

The primary model output is a list of triangles, their maximum, minimum and average temperature at all model depths (over a time range specified by the user), and the depth at which water ice would be stable. The water ice stability depth is based on models developed by Schorghofer and Taylor [9] and assumes a temperature dependent diffusion coefficient. The nominally reported ice depth value is the depth to which ice loss would slow to 1m/Gyr. From the maximum temperature, a companion code can calculate stability of any volatile over any length of time provided the sublimation enthalpy and triple pint pressure and temperature of that compound (as was used in Paige et al., 2013 for Mercury). The model can also be made to output temperatures at all depths and all times, as well as surface visible and thermal insolation.

References:

[1] Feldman, W. C et al (1998). *Science*, *281*(5382), 1496-1500. [2] Arnold, J. R. (1979). JGR Solid Earth, *84*(B10), 5659-5668. [3] Paige, D. A et al. (2010). S*cience*, *330*(6003), 479-482. [4] Siegler, M. A et al. (2016). Lunar true polar wander inferred from polar hydrogen. *Nature*, *531*(7595), 480-484. [5] Schorghofer, N., & Williams, J. P. (2020). *The Planetary Science Journal*, *1*(3), 54. [6] Paige, D. A et al. (2013). *Science*, *339*(6117), 300-303. [7] Hayne, P. et al. (2017) *JGR,*122, 2371-2400. [8] Martinez, A., & Siegler, M. A. (2021). JGR *Planets*, *126*(10), e2021JE006829. [9] Schorghofer, N., & Taylor, G. J. (2007) JGR *Planets*, *112*(E2).